Chapter 4

LONGITUDINAL VEHICLE DYNAMICS

The control of longitudinal vehicle motion has been pursued at many different levels by researchers and automotive manufacturers. Common systems involving longitudinal control available on today's passenger cars include cruise control, anti-lock brake systems and traction control systems. Other advanced longitudinal control systems that have been the topic of intense research include radar-based collision avoidance systems, adaptive cruise control systems, individual wheel torque control with active differentials and longitudinal control systems for the operation of vehicles in platoons on automated highway systems.

This chapter presents dynamic models for the longitudinal motion of the vehicle. The two major elements of the longitudinal vehicle model are the vehicle dynamics and the powertrain dynamics. The vehicle dynamics are influenced by longitudinal tire forces, aerodynamic drag forces, rolling resistance forces and gravitational forces. Models for these forces are discussed in section 4.1. The longitudinal powertrain system of the vehicle consists of the internal combustion engine, the torque converter, the transmission and the wheels. Models for these components are discussed in section 4.2.

4.1 LONGITUDINAL VEHICLE DYNAMICS

Consider a vehicle moving on an inclined road as shown in Figure 4-1. The external longitudinal forces acting on the vehicle include aerodynamic drag forces, gravitational forces, longitudinal tire forces and rolling resistance forces. These forces are described in detail in the sub-sections that follow.

R. Rajamani, *Vehicle Dynamics and Control*, Mechanical Engineering Series,
DOI 10.1007/978-1-4614-1433-9_4, © Rajesh Rajamani 2012

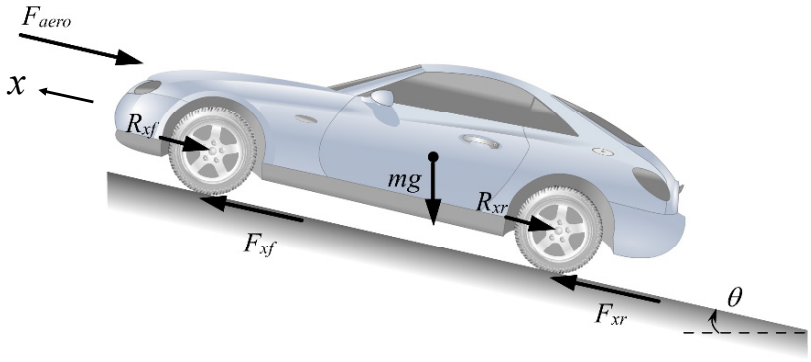

Figure 4-1. Longitudinal forces acting on a vehicle moving on an inclined road

A force balance along the vehicle longitudinal axis yields

$$m\ddot{x} = F_{xf} + F_{xr} - F_{aero} - R_{xf} - R_{xr} - mg\sin(\theta) \tag{4.1}$$

where

F_{xf} is the longitudinal tire force at the front tires

F_{xr} is the longitudinal tire force at the rear tires

F_{aero} is the equivalent longitudinal aerodynamic drag force

R_{xf} is the force due to rolling resistance at the front tires

R_{xr} is the force due to rolling resistance at the rear tires

m is the mass of the vehicle

g is the acceleration due to gravity

θ is the angle of inclination of the road on which the vehicle is traveling

The angle θ is defined to be positive clockwise when the longitudinal direction of motion x is towards the left (as in Figure 4-1). It is defined to be positive counter clockwise when the longitudinal direction of motion x is towards the right.

4.1.1 Aerodynamic drag force

The equivalent aerodynamic drag force on a vehicle can be represented as

$$F_{aero} = \frac{1}{2}\rho C_d A_F (V_x + V_{wind})^2 \tag{4.2}$$

where ρ is the mass density of air, C_d is the aerodynamic drag coefficient, A_F is the frontal area of the vehicle, which is the projected area of the vehicle in the direction of travel, $V_x = \dot{x}$ is the longitudinal vehicle velocity, V_{wind} is the wind velocity (positive for a headwind and negative for a tailwind).

Atmospheric conditions affect air density ρ and hence can significantly affect aerodynamic drag. The commonly used standard set of conditions to which all aerodynamic test data are referred to are a temperature of 15 ^{o}C and a barometric pressure of 101.32 kPa (Wong, 2001). The corresponding mass density of air ρ may be taken as 1.225 kg/m^3.

The frontal area A_F is in the range of 79-84 % of the area calculated from the vehicle width and height for passenger cars (Wang, 2001). According to Wang, 2001, the following relationship between vehicle mass and frontal area can be used for passenger cars with mass in the range of 800-2000 kg:

$$A_f = 1.6 + 0.00056(m - 765) \tag{4.3}$$

The aerodynamic drag coefficient C_d can be roughly determined from a coast-down test (White and Korst, 1972). In a coast down test, the throttle angle is kept at zero and the vehicle is allowed to slow under the effects of aerodynamic drag and rolling resistance. Since there is neither braking nor throttle angle inputs, the longitudinal tire force under these conditions is small and can be assumed to be zero. The road is assumed to be level with $\theta = 0$ and the wind velocity V_{wind} is assumed to be zero.

Under these conditions, the longitudinal dynamics equation can be re-written as

$$-m\frac{dV_x}{dt} = \frac{1}{2}\rho V_x^{\,2} A_F C_d + R_x \tag{4.4}$$

or

$$-\frac{dV_x}{\frac{\rho A_F C_d V_x^{\,2}}{2m}+\frac{R_x}{m}}=dt \tag{4.5}$$

Integrating equation (4.5), assuming an initial longitudinal velocity of V_0, one obtains (White and Korst, 1972)

$$t=\left[\frac{2m^2}{\rho A_F C_d R_x}\right]^{1/2}\left\{\tan^{-1}\left[V_o\left(\frac{\rho A_F C_d}{2R_x}\right)^{1/2}\right]-\tan^{-1}\left[V_x\left(\frac{\rho A_F C_d}{2R_x}\right)^{1/2}\right]\right\} \tag{4.6}$$

Let the total time for the vehicle to coast-down to a stop be $t=T$. Then, non-dimensionalizing using the parameter

$$\beta=V_o\left(\frac{\rho A_F C_d}{2R_x}\right)^{1/2} \tag{4.7}$$

yields

$$\frac{V_x}{V_o}=\frac{1}{\beta}\tan\left[\left(1-\frac{t}{T}\right)\tan^{-1}(\beta)\right] \tag{4.8}$$

In equation (4.8), V_x and t can be measured and the initial velocity V_0 is known. Equation (4.8) represents a one-parameter family, in β, of curves in which non-dimensional velocity $\frac{V_x}{V_o}$ can be plotted against non-dimensional time $\frac{t}{T}$. From such a plot, the value of β for a particular vehicle can be obtained.

Once β has been obtained from equation (4.8), then the following algebraic expressions can be used to calculate the rolling resistance and drag coefficient (White and Korst, 1972):

$$C_d = \frac{2m\beta \tan^{-1}(\beta)}{V_o T \rho A_F} \tag{4.9}$$

$$R_x = \frac{V_o m \tan^{-1}(\beta)}{\beta T} \tag{4.10}$$

These algebraic expressions are obtained by substitution of the final and initial values of time and velocity in equation (4.6) (White and Korst, 1972).

4.1.2 Longitudinal tire force

The longitudinal tire forces F_{xf} and F_{xr} are friction forces from the ground that act on the tires.

Experimental results have established that the longitudinal tire force generated by each tire depends on

a) the slip ratio (defined below),
b) the normal load on the tire and
c) the friction coefficient of the tire-road interface.

The vertical force on a tire is called the tire normal load. The normal load on a tire

a) comes from a portion of the weight of the vehicle
b) is influenced by fore-aft location of the c.g., vehicle longitudinal acceleration, aerodynamic drag forces and grade of the road.
Section 4.1.5 describes calculation of the tire normal loads.

Slip Ratio

The difference between the actual longitudinal velocity at the axle of the wheel V_x and the equivalent rotational velocity $r_{eff}\omega_w$ of the tire is called longitudinal slip. In other words, longitudinal slip is equal to $r_{eff}\omega_w - V_x$. *Longitudinal slip ratio* is defined as

$$\sigma_x = \frac{r_{eff}\omega_w - V_x}{V_x} \text{ during braking} \tag{4.11}$$

$$\sigma_x = \frac{r_{eff}\omega_w - V_x}{r_{eff}\omega_w} \text{ during acceleration} \tag{4.12}$$

An explanation of why longitudinal tire force depends on the slip ratio is provided in section 4.1.3. A more complete understanding of the influence of all three variables – slip ratio, normal force and tire-road friction coefficient – on tire force can be obtained by reading Chapter 13 of this book.

If the friction coefficient of the tire-road interface is assumed to be 1 and the normal force is assumed to be a constant, the typical variation of longitudinal tire force as a function of the slip ratio is shown in Figure 4-2.

As can be seen from the figure, in the case where longitudinal slip ratio is small (typically less than 0.1 on dry surface), as it is during normal driving, the longitudinal tire force is found to be proportional to the slip ratio. The tire force in this small-slip region can then be modeled as

$$F_{xf} = C_{\sigma f}\sigma_{xf} \tag{4.13}$$

$$F_{xr} = C_{\sigma r}\sigma_{xr} \tag{4.14}$$

where $C_{\sigma f}$ and $C_{\sigma r}$ are called the longitudinal tire stiffness parameters of the front and rear tires respectively.

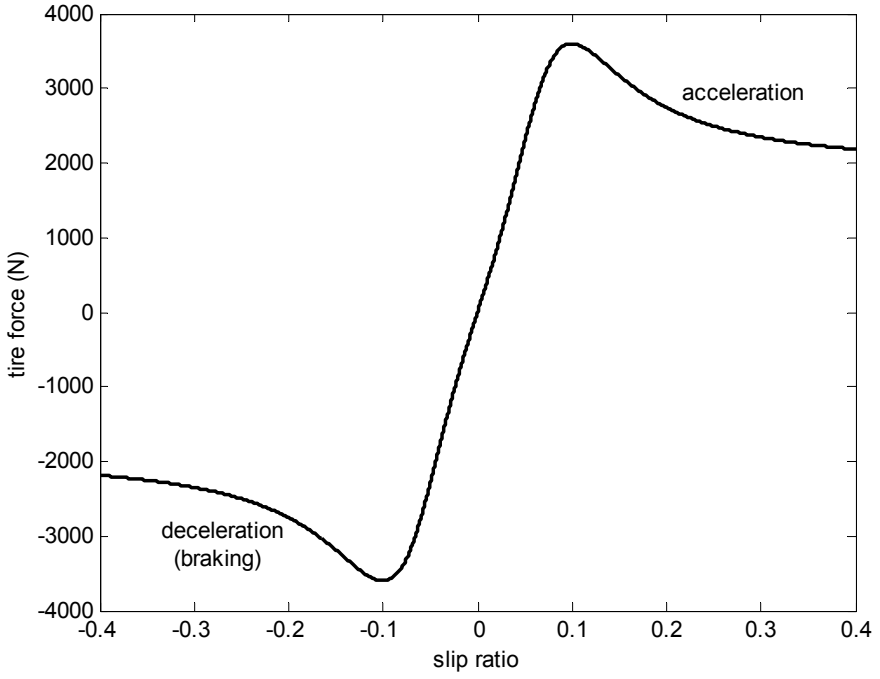

Figure 4-2. Longitudinal tire force as a function of slip ratio

If the longitudinal slip ratio is not small or if the road is slippery, then a nonlinear tire model needs to be used to calculate the longitudinal tire force. The Pacejka "Magic Formula" model or the Dugoff tire model can be used to model tire forces in this case (Pacejka and Bakker, 1993, Pacejka, 1996 and Dugoff, et. al., 1969). These models are discussed in detail in Chapter 13 of this book.

4.1.3 Why does longitudinal tire force depend on slip ?

A rough explanation of why the longitudinal tire force depends on slip ratio can be seen from Figure 4-3.

The lower portion of Figure 4-3 shows a schematic representation of deformation of the tread elements of the tire. The tread elements are modeled as a series of independent springs that undergo longitudinal deformation and resist with a constant longitudinal stiffness. Such a model of the tire is called a "brush" model or an "elastic foundation" model (Pacejka, 1991, Dixon, 1991).

Let the longitudinal velocity of the wheel be V_x and its rotational velocity be ω_w. Then the net velocity at the treads, as shown in Figure 4-3 is $r_{eff}\omega_w - V_x$.

The tire on a vehicle deforms due to the normal load on it and makes contact with the road over a non-zero footprint area called the contact patch (see Figure 13-1 of this book).

First, consider the case where the wheel is a driving wheel, for example, the front wheels in a front-wheel drive vehicle. In this case, since the wheel is a driving wheel, $r_{eff}\omega_w > V_x$. Hence the net velocity of the treads is in a direction opposite to that of the longitudinal velocity of the vehicle. Assume that the slip $r_{eff}\omega_w - V_x$ is small. Then there is a region of the contact patch where the tread elements do not slide with respect to the ground (called the "static region" in Figure 4-3). As the tire rotates and a tread element enters the contact patch, its tip which is in contact with the ground must have zero velocity. This is because there is no sliding in the static region of the contact patch. The top of the tread element moves with a velocity of $R\omega_w - V_x$. Hence the tread element will bend forward as shown in Figure 4-3 and the bending will be in the direction of the longitudinal direction of motion of the vehicle. The maximum bending deflection of the tread is proportional to the slip velocity $r_{eff}\omega_w - V_x$ and to the time duration for which the tread element remains in the contact patch. The time duration in the contact patch is inversely proportional to the rotational velocity $r_{eff}\omega_w$. Hence the maximum

deflection of the tread element is proportional to the ratio of slip to absolute velocity i.e. proportional to the slip ratio $\frac{r_{eff}\omega_w - V_x}{r_{eff}\omega_w}$.

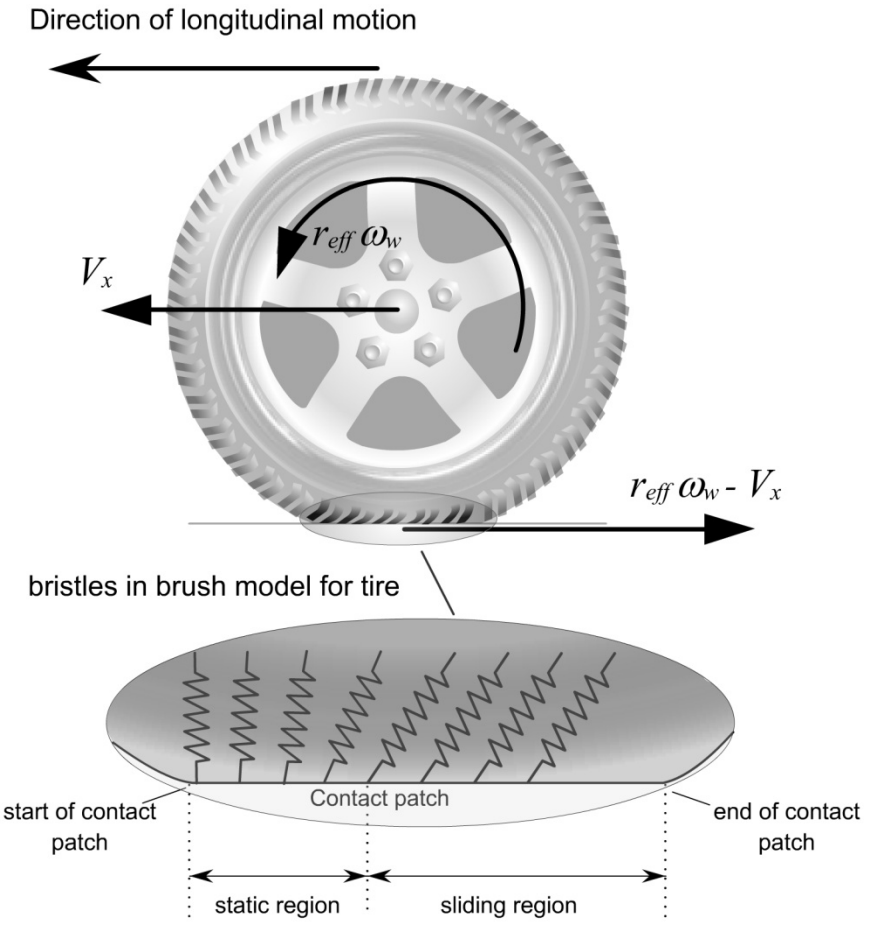

Figure 4-3. Longitudinal force in a driving wheel

Thus the net longitudinal force on the tires from the ground is in the forward direction in the case of a driving wheel and is proportional to the slip ratio of the wheel.

In the case where the tire is on a driven wheel, the longitudinal velocity is greater than the rotational velocity $(V_x > r_{eff}\omega_w)$. In this case the net velocity at the treads is in the forward direction and hence the bristles on the tire will bend backwards. Hence the tire force on the driven wheel is in a

direction opposite to that of the vehicle's longitudinal velocity. Again, for small slip ratio, the tire force will be proportional to slip ratio.

4.1.4 Rolling resistance

As the tire rotates, both the tire and the road are subject to deformation in the contact patch. The road is of course much stiffer and so its deformation can be neglected. But the tire is elastic and new material from the tire continuously enter the contact patch as the tire rotates. Due to the normal load, this material is deflected vertically as it goes through the contact patch and then springs back to its original shape after it leaves the contact patch. Due to the internal damping of the tire material, the energy spent in deforming the tire material is not completely recovered when the material returns to its original shape. This loss of energy can be represented by a force on the tires called the rolling resistance that acts to oppose the motion of the vehicle.

The loss of energy in tire deformation also results in a non-symmetric distribution of the normal tire load over the contact patch. When the tires are static (not rotating), then the distribution of the normal load F_z in the contact patch is symmetric with respect to the center of the contact patch. However, when the tires are rotating, the normal load distribution is non-symmetric, as shown in Figure 4-4.

Imagine the tire being represented by a series of independent springs which resist vertical deformation, as shown in Figure 4-4. As each spring element enters the contact patch, it undergoes vertical deformation. The vertical deformation of the spring reaches its maximum at the center of the contact patch and goes back to zero at the end of the contact patch. If these springs were purely elastic and had no viscous dissipation, then the normal load on the contact patch would be symmetric. But, due to viscous dissipation, the force required to compress the springs in the first half of the contact patch is not fully recovered in the second half of the contact patch. Hence the normal load is not symmetric but is larger in the forward half of the contact patch. This asymmetric normal load distribution is shown in Figure 4-4.

Hence, when the tires are rotating, the resultant normal load F_z moves forward by a distance Δx, as shown in Figure 4-5.

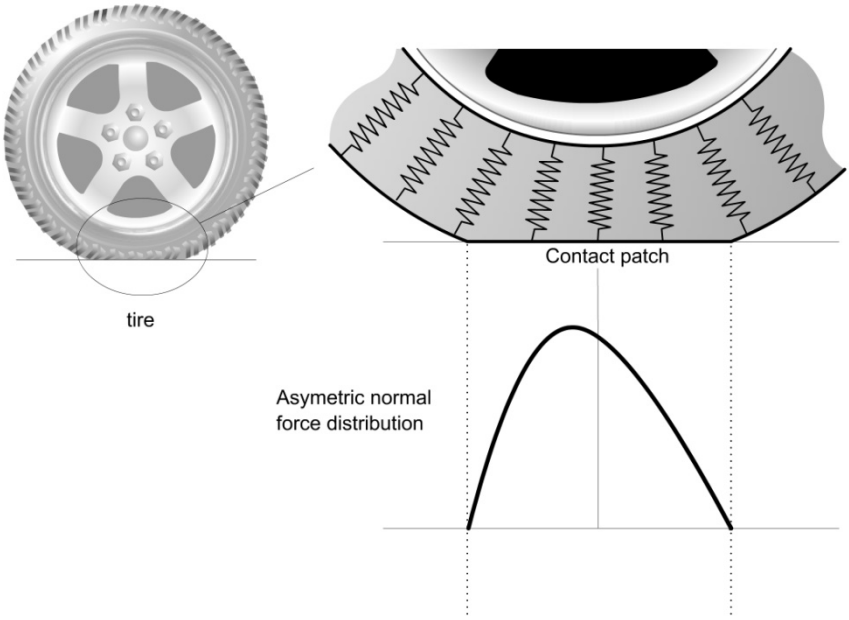

Figure 4-4. Asymmetric normal load distribution on the contact patch

Typically, the rolling resistance is modeled as being roughly proportional to the normal force on each set of tires i.e.

$$R_{xf} + R_{xr} = f(F_{zf} + F_{zr}) \tag{4.15}$$

where f is the rolling resistance coefficient. To see why this approximation is made for the rolling resistance force, consider the action of the normal load and rolling resistance forces shown in Figure 4-5.

The moment $F_z(\Delta x)$ due to the offset normal load is balanced by the moment due to the rolling resistance force $R_x r_{stat}$, where r_{stat} is the statically loaded radius of the tire. Hence

$$R_x = \frac{F_z(\Delta x)}{r_{stat}} \tag{4.16}$$

The variable Δx is not easily measured and therefore R_x is simply modeled as being proportional to F_z with a proportionality constant f.

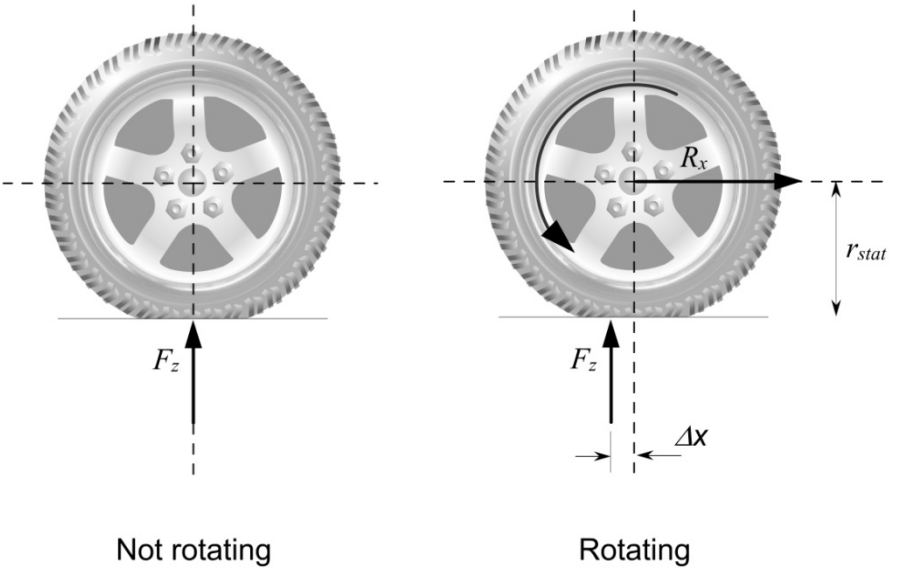

Figure 4-5. Description of rolling resistance

The value of the rolling resistance coefficient f varies in the range 0.01 to 0.04. A value of 0.015 is typical for passenger cars with radial tires (Wong, 2001).

4.1.5 Calculation of normal tire forces

In addition to the total weight of the vehicle, the normal load on the tires is influenced by

a) fore-aft location of the c.g.
b) longitudinal acceleration of the vehicle
c) aerodynamic drag forces on the vehicle
d) grade (inclination) of the road

The normal force distribution on the tires can be determined by assuming that the net pitch torque on the vehicle is zero. In other words, the pitch angle of the vehicle is assumed to have reached a steady state value. Define the following variables

h the height of the c.g. of the vehicle

h_{aero} the height of the location at which the equivalent aerodynamic force acts

ℓ_f the longitudinal distance of the front axle from the c.g. of the vehicle

ℓ_r the longitudinal distance of the rear axle from the c.g. of the vehicle

r_{eff} the effective radius of the tires

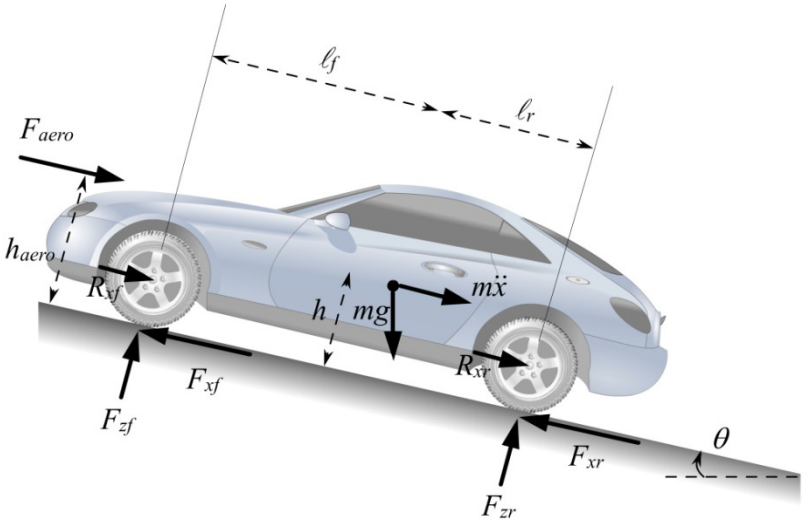

Figure 4-6. Calculation of normal tire loads

Taking moments about the contact point of the rear tire in Figure 4-6

$$F_{zf}(\ell_f + \ell_r) + F_{aero}h_{aero} + m\ddot{x}h + mgh\sin(\theta) - mg\ell_r\cos(\theta) = 0$$

Solving for F_{zf} yields

$$F_{zf} = \frac{-F_{aero}h_{aero} - m\ddot{x}h - mgh\sin(\theta) + mg\ell_r\cos(\theta)}{\ell_f + \ell_r} \tag{4.17}$$

Taking moments about the contact point of the front tire

$$F_{zr}(\ell_f + \ell_r) - F_{aero}h_{aero} - m\ddot{x}h - mgh\sin(\theta) - mg\ell_f\cos(\theta) = 0$$

Solving for F_{zr} yields

$$F_{zr} = \frac{F_{aero}h_{aero} + m\ddot{x}h + mgh\sin(\theta) + mg\ell_f\cos(\theta)}{\ell_f + \ell_r} \tag{4.18}$$

Hence, as the vehicle accelerates, the normal load on the front tires decreases whereas the normal load on the rear tires increases.

4.1.6 Calculation of effective tire radius

The effective tire radius r_{eff} is the value of the radius which relates the rotational angular velocity of the wheel ω_w to the linear longitudinal velocity of the wheel V_{eff} as it moves through the contact patch of the tire with the ground.

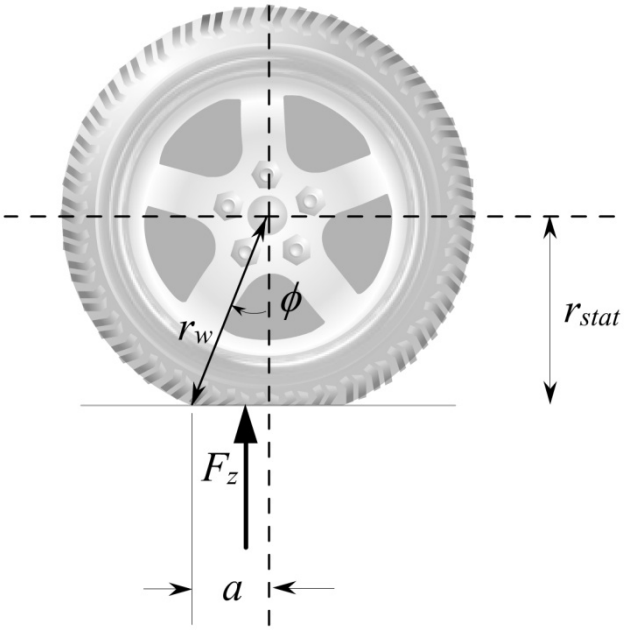

Figure 4-7. Calculation of effective tire radius

If the rotational speed of the wheel is ω_w, the linear equivalent of the rotational speed of the tire is $V_{eff} = r_{eff}\omega_w$ (Kiencke and Nielsen, 2000).

As shown in Figure 4-7, let $2a$ be the longitudinal length of the contact patch and ϕ be the angle made by the radial line joining the center of the wheel to the end of the contact patch. Let t be the duration of time taken by an element of the tire to move through half the contact patch. Then (Kiencke and Nielsen, 2000)

$$V_{eff} = r_{eff}\omega_w = \frac{a}{t} \tag{4.19}$$

At the same time, the rotational speed of the wheel is

$$\omega_w = \frac{\phi}{t} \tag{4.20}$$

Hence

$$r_{eff} = \frac{a}{\phi} \tag{4.21}$$

The static tire radius is the difference between the undeformed radius of the tire r_w and the static vertical deflection of the tire:

$$r_{stat} = r_w - \frac{F_z}{k_t} \tag{4.22}$$

where k_t is the vertical tire stiffness.

From the geometric relationships seen in Figure 4-7

$$r_{stat} = r_w \cos(\phi) \tag{4.23}$$

$$a = r_w \sin(\phi) \tag{4.24}$$

Hence the effective tire radius is given by

$$r_{eff} = \frac{\sin\left\{\cos^{-1}\left(\frac{r_{stat}}{r_w}\right)\right\}}{\cos^{-1}\left(\frac{r_{stat}}{r_w}\right)} r_w \tag{4.25}$$

Note that since $r_{eff} = \frac{\sin(\phi)}{\phi} r_w$, $r_{eff} < r_w$ and that since $r_{eff} = \frac{\tan(\phi)}{\phi} r_{stat}$, $r_{eff} > r_{stat}$. Thus

$$r_{stat} < r_{eff} < r_w \tag{4.26}$$

4.2 DRIVELINE DYNAMICS

In the previous section, we saw that the longitudinal motion equation for the vehicle is of the type

$$m\ddot{x} = F_{xf} + F_{xr} - R_{xf} - R_{xr} - F_{aero} - mg\sin(\theta) \tag{4.27}$$

where F_{xf} and F_{xr} are the longitudinal tire forces. The longitudinal tire forces on the driving wheels are the primary forces that help the vehicle move forward. These forces depend on the difference between the rotational wheel velocity $r_{eff}\omega_w$ and the vehicle longitudinal velocity $\dot{x}$. The wheel rotational velocity ω_w is highly influenced by the driveline dynamics of the vehicle. The major components of a driveline are shown in Figure 4-8 below. The flow of power and the direction of loads on the components is shown in Figure 4-9.

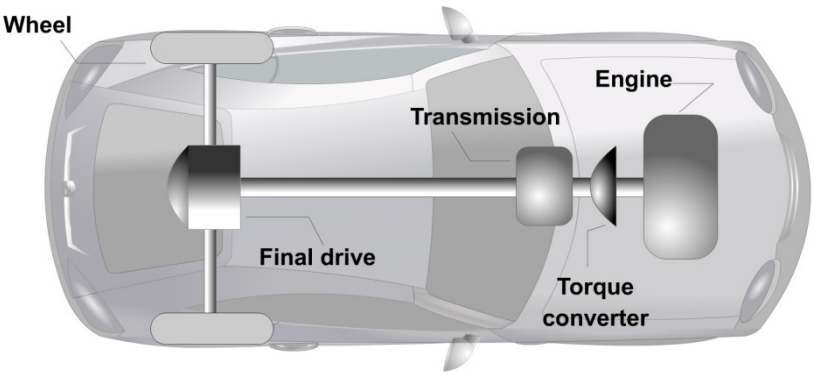

Figure 4-8. Components of a front-wheel drive vehicle powertrain

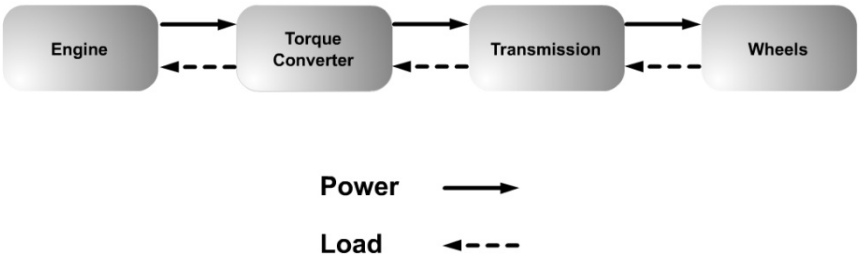

Figure 4-9. Power flow and loads in vehicle drivetrain

4.2.1 Torque converter

The torque converter is a type of fluid coupling that connects the engine to the transmission. If the engine is turning slowly, such as when the car is idling at a stoplight, the amount of torque passed through the torque converter is very small, so keeping the car still requires only a light pressure on the brake pedal.

In addition to allowing the car come to a complete stop without stalling the engine, the torque converter gives the car more torque when it accelerates out of a stop. Modern torque converters can multiply the torque of the engine by two to three times. This effect only happens when the engine is turning much faster than the transmission. At higher speeds, the transmission catches up to the engine, eventually moving at *almost* the same speed. Ideally, though, the transmission should move at exactly the same speed as the engine, because the difference in speed wastes power. To counter this effect, many cars have a torque converter with a lockup clutch. When the two halves of the torque converter get up to speed, this clutch locks them together, eliminating the slippage and improving efficiency.

The torque converter is typically unlocked as soon as the driver removes his/her foot from the accelerator pedal and steps on the brakes. This allows the engine to keep running even if the driver brakes to slow the wheels down.

The major components of the torque converter are a pump, a turbine and the transmission fluid. The fins that make up the pump of the torque converter are attached to the flywheel of the engine. The pump therefore turns at the same speed as the engine. The turbine is connected to the transmission and causes the transmission to spin at the same speed as the turbine, this basically moves the car. The coupling between the turbine and the pump is through the transmission fluid. Torque is transmitted from the pump to the turbine of the torque converter.

Torque converter modeling (both physically based and input-output data based) has been studied by various researchers (see, for example, Kotwicki, 1982, Tugcu, et. al., 1986, Runde, 1986). The static model of Kotwicki (1982) is desirable for control because of its simplicity. It has a reasonable agreement with experimental data for a fairly wide range of operating conditions. This model is a quadratic regression fit of the data from a simple experiment, which involves measuring only the input and output speeds and torques of the torque converter. For the torque converter in Kotwicki (1982), the model expressions are as outlined below.

Let T_p and T_t be pump and turbine torques and $\omega_p (= \omega_e)$ and ω_t be pump and turbine speeds. For converter mode (i.e. $\omega_t / \omega_p < 0.9$), the pump and turbine torques are given by

$$T_p = 3.4325es - 3\omega_p{}^2 + 2.2210\text{x}10^{-3}\omega_p\omega_t - 4.6041\text{x}10^{-3}\omega_t{}^2 \tag{4.28}$$

$$T_t = 5.7656\text{x}10^{-3}\omega_p{}^2 + 0.3107\text{x}10^{-3}\omega_p\omega_t - 5.4323\text{x}10^{-3}\omega_t{}^2 \tag{4.29}$$

For fluid coupling mode (i.e. $\omega_t / \omega_p \geq 0.9$), the pump and turbine torques are given by

$$\begin{aligned} T_p &= T_t \\ &= -6.7644\text{x}10^{-3}\omega_p{}^2 + 32.0024\text{x}10^{-3}\omega_p\omega_t - 25.2441\text{x}10^{-3}\omega_t{}^2 \end{aligned} \tag{4.30}$$

The above equations assume SI units.

The input-output schematic of the torque converter model is shown below in Figure 4-10.

Figure 4-10. Schematic of torque converter model

When the torque converter is locked, as in the third or higher gears, the pump torque is equal to the turbine torque. The pump torque can be calculated in this case by calculating the load on the engine from the wheels and the transmission. This calculation is shown in section 5.5.1.

4.2.2 Transmission dynamics

Let R be the gear ratio of the transmission. The value of R depends on the operating gear and includes the final gear reduction in the differential. In general, $R < 1$ and increases as the gear shifts upwards.

The schematic of the transmission model is shown in Figure 4-11. The turbine torque T_t is the input torque to the transmission. Let the torque transmitted to the wheels be T_{wheels}. At steady state operation under the first, second or higher gears of the transmission, the torque transmitted to the wheels is

$$T_{wheels} = \frac{1}{R} T_t \tag{4.31}$$

The relation between the transmission and wheel speeds is

$$\omega_t = \frac{1}{R} \omega_w \tag{4.32}$$

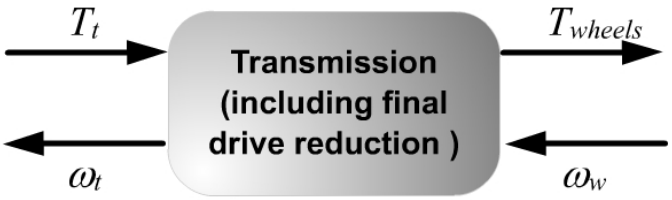

Figure 4-11. Schematic of transmission model

The steady state gear ratio R depends on the operating gear. The operating gear is determined by a gear shift schedule that depends on both the transmission shaft speed and the throttle opening (with fully open throttle angle being counted as 90 degrees). Figure 4-12 shows example up shift and down shift schedules for a 5-speed automatic transmission. Note that the up-shift for each gear change occurs at higher speeds as the throttle angle input from the driver is higher (i.e. the driver is demanding higher torque).

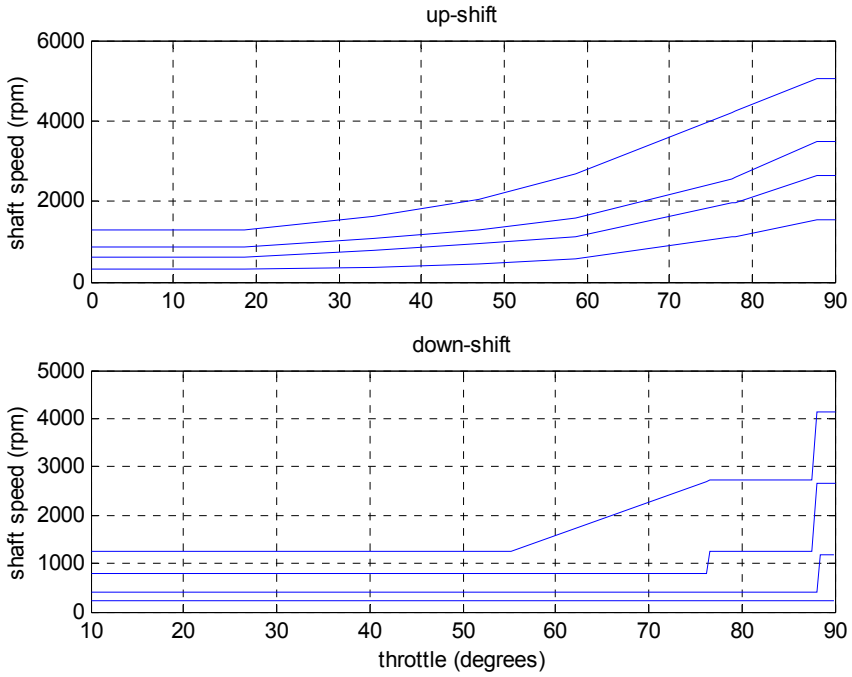

Figure 4-12. Example up shift and down shift schedules for an automatic transmission

Equations describing the dynamics *during* a gear change are complex and can be found in Cho and Hedrick, 1989. An alternative is to replace equations (4.31) and (4.32) by the following 1st order equations *during* a gear change:

$$\tau \dot{T}_{wheel} + T_{wheel} = \frac{1}{R} T_t \tag{4.33}$$

$$\tau \dot{\omega}_t + \omega_t = \frac{\omega_w}{R} \tag{4.34}$$

Equations (4.33) is initialized with $T_{wheel} = 0$ at the instant that the gear change is initiated. R is the gear ratio at the new gear into which the transmission shifts. ω_t is initialized at $\frac{1}{R_{old}} \omega_w$ where R_{old} is the old gear ratio.

The gear change is assumed to be complete when T_{wheel} and ω_t converge to $\frac{1}{R}T_t$ and $\frac{\omega_w}{R}$ within a threshold value. Once the gear change is complete, equations (4.31) and (4.32) can be used again to represent the transmission.

4.2.3 Engine dynamics

The engine rotational speed dynamics can be described by the equation

$$I_e\dot{\omega}_e = T_i - T_f - T_a - T_p \tag{4.35}$$

where T_i is the engine combustion torque, T_f are the torque frictional losses, T_a is the accessory torque and T_p is the pump torque and represents the load on the engine from the torque converter.

Using the notation

$$T_e = T_i - T_f - T_a \tag{4.36}$$

to represent the net engine torque after losses, we have

$$I_e\dot{\omega}_e = T_e - T_p \tag{4.37}$$

The net engine torque T_e depends on the dynamics in the intake and exhaust manifold of the engine and on the accelerator input from the driver. Engine models are discussed in Chapter 9 for both SI and diesel engines and describe how T_e can be calculated. T_p is pump torque and is obtained from equations (4.28) and (4.30) of the torque converter.

The input-output schematic of the engine inertia model is shown in Figure 4-13.

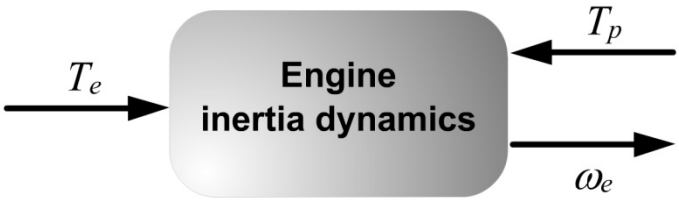

Figure 4-13. Schematic of engine inertia model

4.2.4 Wheel Dynamics

For the driving wheels (for example, the front wheels in a front-wheel driven car), the dynamic equation for the wheel rotational dynamics is

$$I_w \dot{\omega}_{wf} = T_{wheel} - r_{eff} F_{xf} \tag{4.38}$$

where ω_{wf}, T_{wheel} and r_{eff} have been defined earlier and F_{xf} is the longitudinal tire force from the front wheels.

For the non-driven wheels

$$I_w \dot{\omega}_{wr} = -r_{eff} F_{xr} \tag{4.39}$$

where F_{xr} is the longitudinal tire force from the rear wheels.

Figure 4-14. Schematic of wheel dynamics

The total longitudinal tire force is given by

$$F_x = F_{xf} + F_{xr} \tag{4.40}$$

Each of the two tire force terms F_{xf} and F_{xr} is a function of the slip ratio at the front and rear wheels respectively (see section 4.1.2). For

calculation of the slip ratio at the front wheels, ω_{wf} should be used, while for the calculation of the slip ratio at the rear wheels ω_{wr} should be used.

Table 4-1. Summary of longitudinal vehicle dynamic equations

Summary of longitudinal vehicle dynamic equations		
Primary Vehicle Dynamic Equation $m\ddot{x} = F_{xf} + F_{xr} - F_{aero} - R_{xf} - R_{xr} - mg\sin(\theta)$		
1	Front longitudinal tire force	$F_{xf} = C_{\sigma f}\sigma_{xf}$ where $\sigma_{xf} = \frac{r_{eff}\omega_{wf} - \dot{x}}{\dot{x}}$ during braking $\sigma_{xf} = \frac{r_{eff}\omega_{wf} - \dot{x}}{r_{eff}\omega_{wf}}$ during acceleration
2	Rear longitudinal tire force	$F_{xr} = C_{\sigma r}\sigma_{xr}$ where $\sigma_{xr} = \frac{r_{eff}\omega_{wr} - \dot{x}}{\dot{x}}$ during braking $\sigma_{xr} = \frac{r_{eff}\omega_{wr} - \dot{x}}{r_{eff}\omega_{wr}}$ during acceleration
3	Rolling resistance	$R_{xf} + R_{xr} = f(F_{zf} + F_{zr})$ where the front normal tire force is $F_{zf} = \frac{-F_{aero}h_{aero} - m\ddot{x}h - mgh\sin(\theta) + mg\ell_r\cos(\theta)}{\ell_f + \ell_r}$ and the rear normal tire force is $F_{zr} = \frac{F_{aero}h_{aero} + m\ddot{x}h + mgh\sin(\theta) + mg\ell_f\cos(\theta)}{\ell_f + \ell_r}$
4	Aerodynamic drag force	$F_{aero} = \frac{1}{2}\rho C_d A_F(\dot{x} + V_{wind})^2$

4.3 CHAPTER SUMMARY

This chapter presented dynamic equations for the longitudinal motion of the vehicle. The two major elements of the longitudinal dynamic model were the vehicle dynamics and the driveline dynamics.

The vehicle dynamic equations were strongly influenced by longitudinal tire forces, aerodynamic drag forces, rolling resistance forces and gravitational forces. These forces were discussed in detail and mathematical models for each of these forces were described.

The longitudinal driveline system of the vehicle consisted of the internal combustion engine, the torque converter, the transmission and the wheels. Dynamic models for these components were discussed.

NOMENCLATURE

F_{xf}	longitudinal tire force at the front tires
F_{xr}	longitudinal tire force at the rear tires
F_{aero}	equivalent longitudinal aerodynamic drag force
R_{xf}	force due to rolling resistance at the front tires
R_{xr}	force due to rolling resistance at the rear tires
m	mass of the vehicle
g	acceleration due to gravity
θ	angle of inclination of the road on which the vehicle is traveling
ω_w	angular velocity of wheel
r_{eff}	effective radius of rotating tire
r_{stat}	static radius of tire
r_w	radius of undeformed tire
F_z	normal load on tire
Δx	longitudinal distance from center of contact patch at which equivalent normal load acts
a	half-length of contact patch
ϕ	subtended half-angle of contact patch

V_x	longitudinal vehicle velocity
V_{wind}	wind velocity
V_{eff}	effective linear velocity of rotating tire $(=r_{eff}\,\omega_w)$
ρ	mass density of air
C_d	aerodynamic drag coefficient
A_F	frontal area of the vehicle
β	parameter related to aerodynamic drag coefficient calculation
σ_x	slip ratio
h	height of c.g. of vehicle
h_{aero}	height at which equivalent aerodynamic drag force acts
ℓ_f	the longitudinal distance of the front axle from the c.g. of the vehicle
ℓ_r	the longitudinal distance of the rear axle from the c.g. of the vehicle
ω_e	rotational engine speed
ω_t	angular speed of turbine on torque converter
T_p	pump torque
T_t	turbine torque
T_{wheels}	torque transmitted to the wheels
ω_w	angular speed of wheel
τ	time constant in gear change dynamics
R	gear ratio
I_e	engine inertia
T_e	net engine torque after losses
ω_{wf} , ω_{wr}	angular speed of front and rear wheels respectively

REFERENCES

Cho, D. and Hedrick, J.K., "Automotive Powertrain Modeling for Control," *ASME Journal of Dynamic Systems, Measurement and Control*, Vol. 111, pp. 568-576, December 1989.

Dugoff, H., Fancher, P.S. and Segal, L., "Tyre performance charecteristics affecting vehicle response to steering and braking control inputs," *Final Report, Contract CST-460*, Office of Vehicle Systems Research, US National Bureau of Standards, 1969.

Kiencke, U. and Nielsen, L., *Automotive Control Systems for Engine, Driveline and Vehicle*, SAE International, ISBN 0-7680-0505-1, 2000.

Kotwicki, A.J., "Dynamic Models for Torque Converter Equipped Vehicles," *SAE Technical Paper Series*, Paper No. 82039, 1982.

Pacejka, H.B. and Bakker, E., "The Magic Formula Tyre Model," *Vehicle System Dynamics*, v 21, Supplement, Tyre Models for Vehicle Dynamics Analysis, p 1-18, 1993

Pacejka, H.B., "The Tyre as a Vehicle Component," *XXVI FISITA Congress*, Prague, June 16-23, 1996.

Tugcu, A.K., Hebbale, K.V., Alexandridis, A.A., and Karmel, A.M., "Modeling and Simulation of the Powertrain Dynamics of Vehicles Equipped with Automatic Tarnsmission," *Proceedings of the Symposium on Simulation of Ground Vehicles and Transportation Systems*, ASME Winter Annual Meeting, Anaheim, December 1986.

Runde, J., "Modeling and Control of an Automatic Transmission," *S.M.M.E. Thesis*, Department of Mechanical Engineering, M.I.T., January 1986.

White, R.A. and Korst, H.H., "The Determination of Vehicle Drag Contributions from Coastdown Tests," *SAE Transactions*, Vol. 81, paper 720099, 1972.

Wong, J.Y., *Theory of Ground Vehicles*, Wiley-Interscience, ISBN 0-471-35461-9, Third Edition, 2001.